Fraction of natural area as main predictor of net CO_2 emissions from cities

Annika Nordbo[1], Leena Järvi[1], Sami Haapanala[1], Curtis R. Wood[2], Timo Vesala[1]

[1]University of Helsinki, Department of Physics

[2]Finnish Meteorological Institute

annika.nordbo -ÅT- helsinki.fi

leena.jarvi -ÅT- helsinki.fi

sami.haapanala -ÅT- helsinki.fi

curtis.wood -ÅT- fmi.fi

timo.vesala -ÅT- helsinki.fi

Nordbo, A., L. Järvi, S. Haapanala, C. R. Wood, and T. Vesala (2012), Fraction of natural area as main predictor of net CO2 emissions from cities, Geophys. Res. Lett., 39, L20802, doi:10.1029/2012GL053087. To view the published open abstract, go to http://dx.doi.org and enter the DOI.

Abstract

Cities account for most anthropogenic greenhouse-gas emissions, CO_2 being most important. We evaluate the net urban contribution to CO_2 emissions by performing a meta-analysis of all available 14 annual CO_2 budget studies. The studies are based on direct flux measurements using the eddy-covariance technique which excludes all strong point sources. We show that the fraction of natural area is the strongest predictor of urban CO_2 budgets, and this fraction can be used as a robust proxy for net urban CO_2 emissions. Up-scaling, based on that proxy and satellite mapping of the fraction of natural area, identifies urban hotspots of CO_2 emissions; and extraction of 56 individual cities corroborates their inventory-based estimates. Furthermore, cities are estimated as carbon-neutral when the natural fraction is about 80%. This fresh view on the importance of cities in climate change treats cities as urban ecosystems: incorporating natural areas like vegetation.

Main text

1. Introduction

Over 70% of global energy-related CO_2 emissions originate from cities [*WEO,* 2008; *Rosenzweig et al.,* 2010], and fossil fuel combustion―in transportation, industry, and housing―is the dominant urban CO_2 source. Besides CO_2 sources, cities typically have green areas that are carbon sinks through photosynthetic uptake. Since over half of global population is city-based (UN, http://esa.un.org/unpd/wup), urban areas are hotspots of greenhouse gas (GHG) emissions and the focus of innovation in climate-change mitigation [*Kennedy et al.,* 2009]. International negotiations are a key part of climate-change mitigation via GHG-emission reductions. These negotiations necessitate quantification of net GHG exchange between surface and atmosphere, especially CO_2. The eddy-covariance method, the only direct way of measuring surface–atmosphere GHG exchange, is widely applied in natural surroundings. Extensive measurement networks have emerged (AmeriFlux [*Baldocchi et al.,* 2001], EuroFlux [*Valentini et al.,* 2000], AsiaFlux [*Mizoguchi et al.,* 2009]), and continental-scale budgets have recently been estimated of biological GHG fluxes for Europe [*Schulze et al.,* 2009] and global terrestrial ecosystem CO_2 uptake [*Beer et al.,* 2010]. Measurements in urban environments have only, during the past year, become extensive enough to enable synthesis of CO_2 exchange at numerous eddy-covariance sites (*Grimmond and Christen,* 2012). Individual local-scale and city-scale budget estimates include both direct emissions from the city and contributions from vegetation: photosynthetic uptake and respirative emissions, which are seldom within inventories. We thus denote estimates from direct flux measurements as ***net urban ecosystem exchange*** **(NUE)**; a counterpart to net ecosystem exchange, used canonically for non-urban fluxes. NUE describes the CO_2 budget of urban 'background activity': including direct emissions from e.g. buildings and traffic; but excluding strong point sources like power stations. This is not disadvantageous, since emissions from such strong point sources are well-described in inventories (Carbon Monitoring and Action, http://carma.org), whereas NUE has remained unresolved until now.

Apart from direct flux measurements, multiple studies have gathered inventories of annual GHG emissions from nations [*Hertwich and Peters,* 2009] or individual urban areas [*Dodman,* 2009; *Kennedy et al.,* 2011] based on consumption statistics. Furthermore, area-specific inventories of CO_2 emissions have been utilized for mapping global emissions based on population densities and night-time lights [*Raupach et al.,* 2010; *Oda and Maksyutov,* 2011], and CO_2 emissions in USA have been down-scaled to a 10 km grid scale [*Gurney et al.,* 2009; *Parshall et al.,* 2010]. These inventory-based methods, as indirect estimations of GHG emissions, have inherent disadvantages: fossil fuels are often not consumed where purchased, population data represent commuting inconsistently, and there is no clear literature consensus whether emissions estimates should be end-use or only from those emissions produced within city borders. Conversely, the definition of NUE is rigorous: it is an *in-situ* measure of the local CO_2 budget, excluding any city-related emissions located outside city borders (e.g. aviation, marine, electricity production, product manufacturing).

We present a meta-analysis of a compilation of 17 annual NUE budgets from direct flux measurements from 14 urban eddy-covariance towers, and analyze the predictors of surface–atmosphere exchange. The fraction of natural area in a city (derived from satellite data) is used as a proxy for estimating regional variation of NUE in parts of North America, Europe, and eastern Asia; and those estimates for particular cities are compared against inventory-based estimates. Here natural fraction means the fraction of land area that is covered by surface types existing in nature (e.g. grass, trees, soil, sand), whereas urban fraction means all non-vegetative, human-constructed elements. Additionally, a natural fraction is conjectured for a carbon-neutral city (annual NUE zero).

2. Data and methods

The eddy-covariance technique is tower-based and the measurements' source area is several hectares: depending on the upwind surface, measurement height, and flow properties [*Vesala et al.,* 2008]. The technique is based on measuring simultaneous turbulent variations in wind and gas concentrations (e.g. CO_2): output typically being 30-minute fluxes. The measurements used in this study (Auxiliary Figure 1, Auxiliary Table 1) represent over 16 000 days' measurements with 58% data coverage (the percentage is typical for the method). Data were processed by original authors with widely-accepted procedures, including quality-screening, the main cause of data-loss. Time series consequently were gap-filled (typical errors are below 5% [*Järvi et al.,* 2012]) to enable annual-sum calculations. Furthermore, typical random errors are under 20% for half-an-hour fluxes [*Aubinet et al.,* 2012; *Nordbo et al.,* 2012], and the random error is assumed negligible for annual sums of NUE. Data coverage at each site is taken into account when analyzing predictors of NUE and non-linear least-squares optimization is used for non-linear fits.

The natural fraction (f_n) is estimated from the urban fraction ($f_u = 1 - f_n$) which can be retrieved from global satellite data. The urban fraction is derived from binary (urban/non-urban), 500-meter-resolution data from the MODIS satellite in 2001–2002 [*Schneider et al.,* 2009, 2010]. Urban area was defined as "a place dominated by built environment"—which includes all non-vegetative, human-constructed elements like buildings, roads, and runways. The mean accuracy of the binary data exceeds 93% [*Schneider et al.,* 2009]. Binary data were converted by us to f_u by aggregating to 4x4 km resolution, each aggregated pixel based on 64 binary values. GHG inventories from 56 urban areas (cities, metropolitan areas, counties) in North America, Europe, and eastern Asia were compiled (Auxiliary Table 2). Corresponding NUE estimates are subsequently retrieved using the 4 km resolution values of f_u within official administrative areas (Database of Global Administrative Areas, www.gadm.org). A pixel is included if the pixel's center is within the administrative area. If beyond 50% of a pixel is water, the pixel is omitted. If administrative areas are below 1000 km^2, f_u data are disaggregated back to 500-meter resolution to minimize edge problems.

3. Results and Discussion

3.1 Predictors of net urban ecosystem exchange

The compilation of direct annual NUE measurements shows that urban areas are sources of CO_2 (Figure 1). Annual emissions are as high as 9.7 kg C m^{-2} yr^{-1} in London [*Helfter et al.,* 2011], which is forty times the typical uptake of grassland [*Soussana et al.,* 2007] and over ten times the global median terrestrial ecosystem uptake [*Beer et al.,* 2010]. The Minnesota site, conversely, is only a very small CO_2 source, since the measurements were carried out in an urban park [*Hiller et al.,* 2011].

The fraction of natural area (f_n) in the source area of the measurements is a robust proxy for annual NUE (coefficient of determination r^2 = 0.84, Figure 1), especially when considering the variety between cities' surface cover and latitude. Previously, non-gapfilled CO_2 fluxes (mostly) from summertime have been compared with vegetation fraction for 18 sites [*Velasco and Roth,* 2010] and with building fraction for 22 sites [*Grimmond and Christen,* 2012]. Five annual CO_2 budgets were compared as a function of vegetation fraction [*Helfter et al.,* 2011], but two of the budgets were based on measurements during one season, and the given exponential fit saturated to an unrealistic value for complete vegetation cover (2.5 kg C m^{-2} yr^{-1}). Population density has a lesser correlation with NUE (r^2 = 0.60, rms 1.13 kg C m^{-2} yr^{-1} Auxiliary Figure 3), although population density is an indicator for energy consumption, perhaps because traffic-fuel demand decreases as population density grows [*Kennedy et al.,* 2009; *Karathodorou et al.,* 2010]. A correlation between annual CO_2 budgets and population density has not been seen before [*Helfter et al.,* 2011].

The strong relationship between NUE and f_n can be explained by the indirect links that f_n has to many factors determining CO_2 release: greater f_n is consistent with a lesser road and population density, which thus limits CO_2 release from fossil-fuel combustion and human respiration [*Moriwaki and Kanda,* 2004]. Greater f_n can also reduce pedestrian and building cooling-needs, e.g. via shading effects of trees [*Simpson,* 2002]. Vegetation itself is also a key NUE component through daytime sequestration of carbon via photosynthesis. The non-linearity of the relationship in Figure 1 comes from the dependency of population density on urban density: population grows exponentially when a dense city becomes even more compact [*Pozzi and Small,* 2005] since cities do not only grow horizontally but also vertically. Furthermore, dense urban living may generate less per-capita GHG emissions compared to rural living, given a similar income level, since urban areas often have lower emissions than the national average [*Brown et al.,* 2009; *Dodman,* 2009] or rural areas [*Parshall et al.,* 2010]. Standard of living is a predictor for CO_2 release, since greater incomes often lead to greater consumption [*Kennedy et al.,* 2009]. Conversely, technological advances—usually a consequence of wealth increase—can decrease the emission intensity of CO_2 per unit GDP: the overall global emission intensity has decreased by 41% from 1971 to 2007 [*International Energy Agency,* 2009].

A minimum f_n requirement for a carbon-neutral city (annual NUE zero) can be interpreted from the fit in Figure 1: cities are net sinks of CO_2 if their natural fraction exceeds about 80%. This value can be used as a first rule-of-thumb estimate in urban planning, among other indicators [*Kennedy et al.,* 2011]. The general definition of a carbon-neutral city suffers from a scoping problem: some definitions require zero carbon emissions, others allow emissions to be balanced by sequestration or export of low-carbon goods [*Kennedy and Sgouridis,* 2011]. In our case, the limit for carbon-neutrality treats the city as an urban ecosystem comprising *in-situ* sinks and sources of CO_2 within the city boundaries. Increasing the natural land area fraction within a city is expected to decrease the CO_2 emissions per unit area, but this is not a general solution for climate-change mitigation: if natural area substitutes previously-occupied buildings, the per-capita emissions might increase, if the living density decreases. Conversely, if an unused urban area (e.g. abandoned car park) is transformed into a vegetated area, then there is an obvious, but small, net gain. Green roofs, to the contrary, are usually a net gain in energy savings [*Sailor et al.,* 2012] and photosynthetic uptake of CO_2.

3.2 Regional estimates for NUE

The strength of f_n as a predictor of NUE provides a means for producing annual NUE estimates based solely on land-cover data, using the relationship in Figure 1. The global f_u is calculated based on satellite observations for North America, Europe, and eastern Asia (Section 2). These areas were chosen for mapping since all-but-one of the flux sites are within these regions and thus the relationship in Figure 1 is assumed to be applicable within these regions. In Europe, high urbanization dominates around the Benelux countries, Germany, and southern England (Figure 2 a). In North America, the north-east coast of USA, the Great Lakes region, Los Angeles, and Florida have conspicuously continuous and high urban fraction (Auxiliary Figure 4a). In eastern Asia, the east coast of China and the Tokyo metropolis have prominently-high urban fractions (Auxiliary Figure 5a).

Mid-Europe and United Kingdom are regions of high NUE in Europe (Figure 2 b). The summed NUE over EU_{25} and EU_{27} (EU countries prior to and after 2007) are 410 Tg C yr^{-1} and 414 Tg C yr^{-1}, from which about 9% can be allocated to human respiration of the whole population. The inventory-based emissions were twice the NUE (767 Tg C yr^{-1} in 2006) [*WEO,* 2008], and NUE is almost four times the uptake of CO_2 by biological fluxes (–102 ± 23 Tg C yr^{-1}, EU_{25}) [*Schulze et al.,* 2009]. The inventory-based emissions and NUE are not intended to coincide, since some inventories include both strong point sources and emissions occurring outside the city borders. Furthermore, NUE includes vegetation uptake, whereas the inventories only include CO_2 emissions and might include emissions of other GHGs.

In North America, the regional distribution of NUE follows that of urban fraction (Auxiliary Figure 4b). The summed NUE is 460 Tg C yr^{-1} for USA_{48} (i.e. all states excluding Alaska and Hawaii). From this, 5% can be allocated to human respiration of the whole population (76.3 kg C yr^{-1} per person [*Moriwaki and Kanda,* 2004]) and about 5% to uptake by urban trees (23 Tg C yr^{-1}) [*Nowak and Crane,* 2002]. In 2006, the inventory-based CO_2 emissions from urban areas in USA were three times the NUE (1228 Tg C yr^{-1}) [*WEO,* 2008].

In eastern Asia, a large area of NUE sink is seen in north-east China where low urban fraction is observed (Auxiliary Figure 5b). Chinese urbanization is characterized by a continuous sprawl as an opposite to the more confined city structures seen in Europe (see also Auxiliary Figure 2). To the contrary, the metropolitan areas of Tokyo, Seoul, Beijing, and Shanghai arise as large CO_2 sources. The NUE of Japan is 77 Tg C yr^{-1}, which is 22% of the country-wide inventory estimate [*Nojiri et al.,* 2012]. An estimate for the whole of China is not given, since the sites in Figure 1 are not representative of China as a whole.

3.3 NUE and inventories of individual cities

The NUE estimates of urban areas are expected to relate to inventories, though they are also expected to be systematically lower (as discussed above). Following this reasoning, a set of 56 GHG inventories from individual cities, or metropolitan areas, was collected in order to conduct an independent comparison against the corresponding NUE estimates (see Auxiliary Table 2). The NUE estimates are lower than the inventory-based GHG emissions for all cases but Prague (slope 0.50, Figure 3). The inclusion of strong point sources in inventories can be seen for example for Rotterdam where over 60% of emissions are due to energy industries. Nevertheless, there is a clear linear dependency ($r^2 = 0.72$, rms = 1.42 kg C m^{-2} yr^{-1}), and 22 out of the 56 cities are net CO_2 sinks. This result corroborates the usability of the proxy of NUE as a function of f_n, and confirms its use as a robust independent check against international inventory studies.

4. Summary and Conclusions

The urban CO_2 budgets (Figure 2, Auxiliary Figures 4 and 5) are the first continental-scale estimations from direct flux measurements. The mapping estimation treats cities as ecosystems, i.e. incorporating vegetation. The mapping is solely from the relationship between the CO_2 budget and the natural land fraction; the 14 eddy-covariance stations are assumed representative at continental scale—resulting in high uncertainties in estimates of annual CO_2 budgets. Direct validation of the continental-scale NUE parameterization is not possible due to the non-existence of another method that could provide CO_2 budgets of urban ecosystems. Nevertheless, the high correspondence of our continental-scale estimates with individual cities' inventory-based estimates (Figure 3) supports the new method's robustness. The inventory-based estimates exceed the parameterized NUE (median ratio 1.33), this is reasonable since NUE lacks strong point sources and includes vegetative uptake.

Direct urban-flux measurements have become comprehensive enough to benefit decision-makers and urban planners. Additional urban CO_2 budget measurements, extending beyond a year, are needed to represent diverse urban morphologies (very high or low f_u) and climates (Asia, Africa, and South America). Until present only short-term urban CH_4 [*Gioli et al.,* 2012] and N_2O [*Famulari et al.,* 2010] campaigns have been under-taken, although their anthropogenic emissions are increasing [*Montzka et al.,* 2012]; the need for long-term flux measurements is clear.

Acknowledgements

For funding we thank the Academy of Finland Centre of Excellence program (project no 1118615), the Academy of Finland project 138328, the Academy of Finland ICOS project (263149), the EU ICOS project (211574), the EU GHG-Europe project (244122) and an EU FP7 grant (ERC 227915). For the satellite surface-cover data we thank Annemarie Schneider. We acknowledge Hotel Torni for providing a platform for eddy-covariance measurements.

Reference list

Aubinet, M., T. Vesala, and D. Papale (Eds.) (2012), *Eddy Covariance - A Practical Guide to Measurement and Data Analysis*, Springer atmospheric sciences, the Netherlands.

Baldocchi, D. et al. (2001), FLUXNET: A new tool to study the temporal and spatial variability of ecosystem-scale carbon dioxide, water vapor, and energy flux densities, *Bull. Am. Meteorol. Soc., 82*, 2415-2434.

Beer, C. et al. (2010), Terrestrial Gross Carbon Dioxide Uptake: Global Distribution and Covariation with Climate, *Science, 329*, 834-838.

Bergeron, O. and I. B. Strachan (2011), CO2 sources and sinks in urban and suburban areas of a northern mid-latitude city, *Atmos. Environ., 45*, 1564-1573.

Brown, M. A., F. Southworth, and A. Sarzynski (2009), The geography of metropolitan carbon footprints, *Policy and Society, 27*, 285-304.

Christen, A., N. C. Coops, B. R. Crawford, R. Kellett, K. N. Liss, I. Olchovski, T. R. Tooke, M. van der Laan, and J. A. Voogt (2011), Validation of modeled carbon-dioxide emissions from an urban neighborhood with direct eddy-covariance measurements, *Atmos. Environ., 45*, 6057-6069.

Coutts, A. M., J. Beringer, and N. J. Tapper (2007), Characteristics influencing the variability of urban CO2 fluxes in Melbourne, Australia*, Atmos. Environ., 41*, 51-62.

Crawford, B., C. S. B. Grimmond, and A. Christen (2011), Five years of carbon dioxide fluxes measurements in a highly vegetated suburban area*, Atmos. Environ., 45*, 896-905.

Dodman, D. (2009), Blaming cities for climate change? An analysis of urban greenhouse gas emissions inventories*, Environ. Urban., 21*, 185-201.

Famulari, D., E. Nemitz, C. Di Marco, G. J. Phillips, R. Thomas, E. House, and D. Fowler (2010), Eddy-covariance measurements of nitrous oxide fluxes above a city*, Agric. For. Meteorol., 150*, 786-793.

Gioli, B., P. Toscano, E. Lugato, A. Matese, F. Miglietta, A. Zaldei, and F. P. Vaccari (2012), Methane and carbon dioxide fluxes and source partitioning in urban areas: The case study of Florence, Italy*, Environ. Pollut., 164*, 125-131.

Grimmond, C. S. B. and A. Christen (2012), Flux measurements in urban ecosystems*, Fluxletter - The newsletter of FLUXNET, 5*, 1-8.

Gurney, K. R., D. L. Mendoza, Y. Zhou, M. L. Fischer, C. C. Miller, S. Geethakumar, and Du Can,Stephane De La Rue (2009), High Resolution Fossil Fuel Combustion CO2 Emission Fluxes for the United States*, Environ. Sci. Technol., 43*, 5535-5541.

Helfter, C., D. Famulari, G. J. Phillips, J. F. Barlow, C. R. Wood, C. S. B. Grimmond, and E. Nemitz (2011), Controls of carbon dioxide concentrations and fluxes above central London*, Atmos. Chem. Phys., 11*, 1913-1928.

Hertwich, E. G. and G. P. Peters (2009), Carbon Footprint of Nations: A Global, Trade-Linked Analysis*, Environ. Sci. Technol., 43*, 6414-6420.

Hiller, R. V., J. P. McFadden, and N. Kljun (2011), Interpreting CO2 Fluxes Over a Suburban Lawn: The Influence of Traffic Emissions*, Bound. -Layer Meteorol., 138*, 215-230.

International Energy Agency (2009), CO2 emissions from fuel combustion*, IEA Statistics*, 1-115.

Järvi, L., A. Nordbo, H. Junninen, A. Riikonen, J. Moilanen, E. Nikinmaa, and T. Vesala (2012), Seasonal and annual variation of carbon dioxide surface fluxes in Helsinki, Finland, in 2006-2010*, Atmos. Chem. Phys. Discuss., 12*, 8355-8396.

Karathodorou, N., D. J. Graham, and R. B. Noland (2010), Estimating the effect of urban density on fuel demand*, Energy Econ., 32*, 86-92.

Kennedy, C., S. Pincetl, and P. Bunje (2011), The study of urban metabolism and its applications to urban planning and design*, Environ. Pollut., 159*, 1965-1973.

Kennedy, C., J. Steinberger, B. Gasson, Y. Hansen, T. Hillman, M. Havranek, D. Pataki, A. Phdungsilp, A. Ramaswami, and G. Villalba Mendez (2009), Greenhouse Gas Emissions from Global Cities*, Environ. Sci. Technol., 43*, 7297-7302.

Kennedy, S. and S. Sgouridis (2011), Rigorous classification and carbon accounting principles for low and Zero Carbon Cities*, Energy Policy, 39*, 5259-5268.

Kordowski, K. and W. Kuttler (2010), Carbon dioxide fluxes over an urban park area*, Atmos. Environ., 44*, 2722-2730.

Mizoguchi, Y., A. Miyata, Y. Ohtani, R. Hirata, and S. Yuta (2009), A review of tower flux observation sites in Asia*, J. For. Res., 14*, 1-9.

Montzka, S. A., E. J. Dlugokencky, and J. H. Butler (2012), Non-CO2 greenhouse gases and climate change*, Nature, 476(7358)*, 43-50.

Moriwaki, R. and M. Kanda (2004), Seasonal and diurnal fluxes of radiation, heat, water vapor, and carbon dioxide over a suburban area*, J. Appl. Meteorol., 43*, 1700-1710.

Nojiri, Y., J. Akagi, E. Hatanaka, Y. Hayabuchi, K. Hirai, T. Oda, A. S. Osako K., and Tamai,A.,White,M. (2012), National Greenhouse Gas Inventory Report of Japan*, Ministry of the Environment, Japan*, 1-608.

Nordbo, A., L. Järvi, S. Haapanala, J. Moilanen, and T. Vesala (2012), Intra-city variation in urban morphology and turbulence structure in Helsinki, Finland*, In review in Bound. -Layer Meteorol.*

Nowak, D. J. and D. E. Crane (2002), Carbon storage and sequestration by urban trees in the USA, *Environ. Pollut., 116*, 381-389.

Oda, T. and S. Maksyutov (2011), A very high-resolution (1 km x 1 km) global fossil fuel CO2 emission inventory derived using a point source database and satellite observations of nighttime lights, *Atmos. Chem. Phys., 11*, 543-556.

Parshall, L., K. Gurney, S. A. Hammer, D. Mendoza, Y. Zhou, and S. Geethakumar (2010), Modeling energy consumption and CO2 emissions at the urban scale: Methodological challenges and insights from the United States, *Energy Policy, 38*, 4765-4782.

Pawlak, W., K. Fortuniak, and M. Siedlecki (2011), Carbon dioxide flux in the centre of Lodz, Poland - analysis of a 2-year eddy covariance measurement data set, *Int. J. Climatol., 31*, 232-243.

Pozzi, F. and C. Small (2005), Analysis of urban land cover and population density in the United States, *Photogramm. Eng. Remote Sensing, 71*, 719-726.

Raupach, M. R., P. J. Rayner, and M. Paget (2010), Regional variations in spatial structure of nightlights, population density and fossil-fuel CO2 emissions, *Energy Policy, 38*, 4756-4764.

Rosenzweig, C., W. Solecki, S. A. Hammer, and S. Mehrotra (2010), Cities lead the way in climate-change action, *Nature, 467*, 909-911.

Sailor, D. J., T. B. Elley, and M. Gibson (2012), Exploring the building energy impacts of green roof design decisions - a modeling study of buildings in four distinct climates, *J. Build Phys., 35*, 372-391.

Schneider, A., M. A. Friedl, and D. Potere (2009), A new map of global urban extent from MODIS satellite data, *Environ. Res. Lett., 4*, 044003.

Schneider, A., M. A. Friedl, and D. Potere (2010), Mapping global urban areas using MODIS 500-m data: New methods and datasets based on 'urban ecoregions', *Remote Sens. Environ., 114*, 1733-1746.

Schulze, E. D. et al. (2009), Importance of methane and nitrous oxide for Europe's terrestrial greenhouse-gas balance, *Nat. Geosci., 2*, 842-850.

Simpson, J. R. (2002), Improved estimates of tree-shade effects on residential energy use*, Energy Build., 34*, 1067-1076.

Soussana, J. F. et al. (2007), Full accounting of the greenhouse gas (CO2, N2O, CH4) budget of nine European grassland sites*, Agric. Eco. Env., 121*, 121-134.

Valentini, R. et al. (2000), Respiration as the main determinant of carbon balance in European forests*, Nature, 404*, 861-865.

Velasco, E. and M. Roth (2010), Cities as Net Sources of CO2: Review of Atmospheric CO2 Exchange in Urban Environments Measured by Eddy Covariance Technique*, Geogr. Comp., 4*, 1238-1259.

Vesala, T., N. Kljun, Ü. Rannik, J. Rinne, A. Sogachev, T. Markkanen, K. Sabelfeld, T. Foken, and M. Y. Leclerc (2008), Flux and concentration footprint modelling: State of the art*, Environ. Pollut., 152*, 653-666.

WEO (2008), Chapter 16: Implications of the reference scenario for the global climate*, In: World Energy Outlook*.

Figures

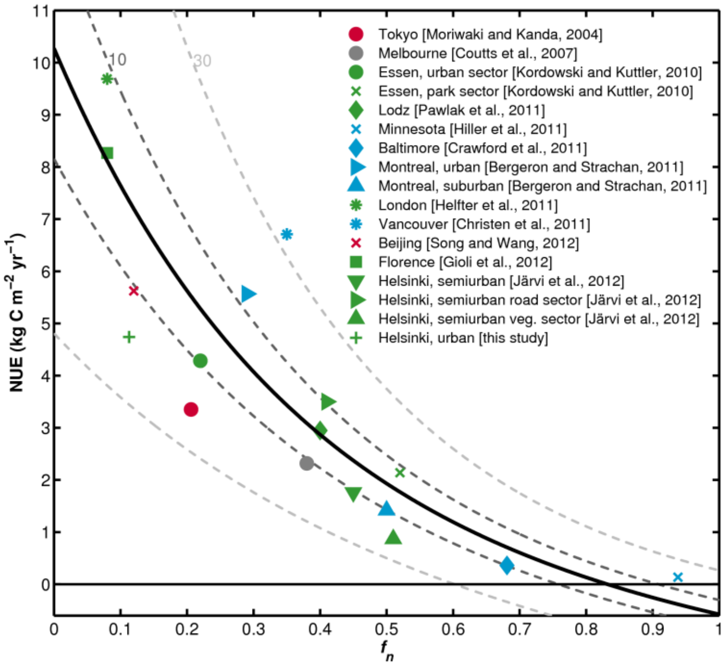

Figure 1. CO_2 exchange versus natural fraction. Net urban ecosystem exchange (NUE) from direct eddy-covariance flux measurements as a function of fraction of natural area (f_n). Shown as colors are: North America (blue), Europe (green), eastern Asia (red), Australia (grey). The weighted fit to all data is NUE = –1.20 kg C m^{-2} yr^{-1} f_n + 0.62 kg C m^{-2} yr^{-1} exp[2.80(1–f_n)], N = 17, r^2 = 0.84, rms = 0.77 kg C m^{-2} yr^{-1}. The dashed lines show confidence levels of fit (%, given in figure). See Auxiliary Table 1 for further detail on the eddy-covariance data.

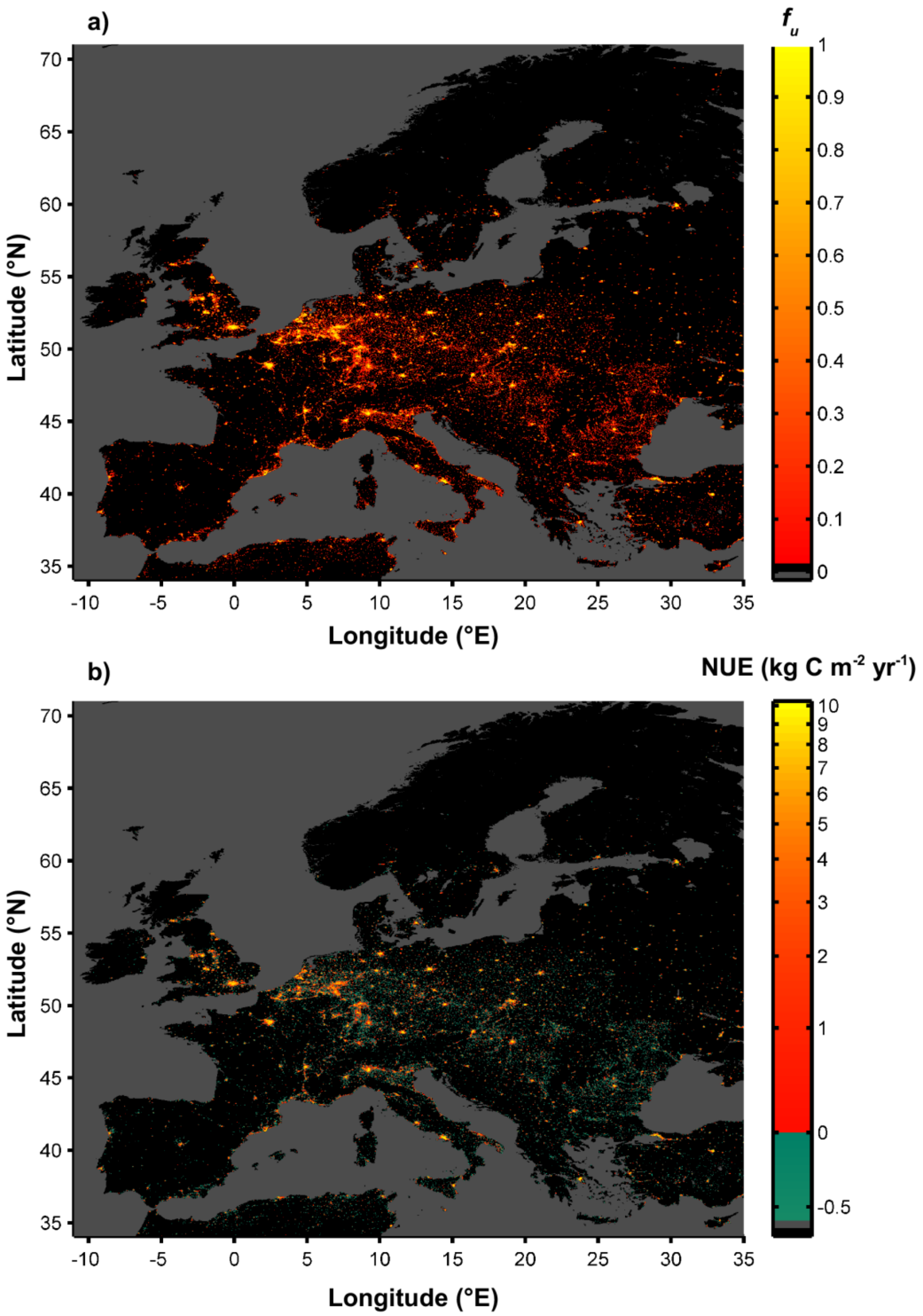

Figure 2. Urbanization and CO_2 budget in Europe. a) Urban fraction (f_u) based on satellite observations, b) Net urban ecosystem exchange (NUE, kg C m^{-2} yr^{-1}) based on robust parameterization as a function of fraction of natural area (Figure 1).

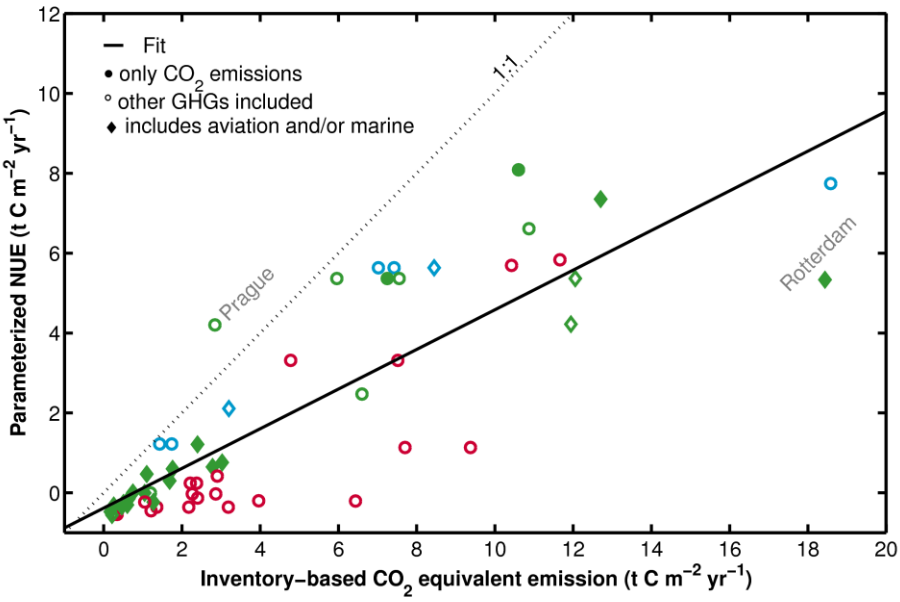

Figure 3. Comparison of NUE and inventory-based estimates. The parameterized net urban ecosystem exchange (NUE, kg C m^{-2} yr^{-1}) is calculated using satellite land-cover data, administrative borders, and the fit in Figure 1. The inventory-based emissions (kg equivalent C m^{-2} yr^{-1}) are listed in Auxiliary Table 2. The inventories contain only CO_2 (filled markers) or all GHGs (open markers); some contain aviation and/or marine emissions (diamond markers). Shown as colors are: North America (blue), Europe (green), eastern Asia (red). The fit is NUE = 0.50 inventory –0.38 kg C m^{-2} yr^{-1}, N = 56, r^2 = 0.72, rms = 1.42 kg C m^{-2} yr^{-1}.

Auxiliary material

1. Auxiliary methods

Sites with eddy-covariance measurements and cities with GHG inventories

A list of 14 eddy-covariance flux towers, that provide 17 annual net urban ecosystem exchange (NUE) estimates, is given in Auxiliary Table 1. The NUE estimates, the fraction of natural area (f_n), the radius of the circle for which f_n was determined (R), and the amount of data are all determined by original authors (exceptions are in the footnote of Auxiliary Table 1). Most of the sites are located in North America and Europe (five each), two are from eastern Asia, and one from Australia (Auxiliary Figure 1). The measurements represent a variety of urban forms comprising for example a highway passing a lawn [*Hiller et al.,* 2011], a suburban district [*Crawford et al.,* 2011], and the densely built-up metropolitan area of London [*Helfter et al.,* 2011].

The values of f_n range from 8% to 94% and they are equal to the vegetative fraction for all but Baltimore and semi-urban Helsinki, but the fraction of non-vegetative surfaces (bare soil) remains <1%. The source area of eddy-covariance measurements depends for instance on the measurement height [*Vesala et al.,* 2008], and thus f_n values per site are given for differently-sized areas around the measurement towers (Auxiliary Table 1). The values of R are shown to give a view of the size of the source area of the NUE estimates, though R is not used in the analysis as such. The data coverage for each site (N, days) was calculated by us based on the reported measurement period and overall data rejection due to quality screening. Only sites with all-year-around measurements were included, but N may be under a year due to quality screening and the separation into different wind direction sectors (see e.g. Essen in Auxiliary Table 1). The data coverage was taken into account in the exponential fit of Figure 1 in the main text by weighting data points by N(Auxiliary Table 1). The fit in is made using the fit-function in MATLAB (*Mathwoks Inc. 2012*). The solution is found by non-linear least-squares optimization, and confidence limits of the fit are provided by the function.

A list of 56 greenhouse gas (GHG) inventories is provided in Auxiliary Table 2. Four main criteria were used in the selection of inventories: population census data must have been provided, the research must have been conducted in the 21st century, the area in concern must have been clearly indicated (as city, metropolitan, or county), and polygons [*GADM,* 2012] for the corresponding area must be available. The latter criterion caused the rejection of several of USA's cities since often only county borders were available. The resulting compilation of cities has a large variation in population: eleven of the cities have over 10 million inhabitants and ten have a population of less than a million. Where possible, an emission value only including the effect of CO_2 is given. Furthermore, if a value for emissions that occur only within city boundaries was available, it was favored over emissions attributable to end-use in cities (including e.g. power generation, air transport, and marine transport). The large spectrum of methodologies behind inventory estimates is not considered a drawback, since our NUE estimates are intended to describe the urban area as an ecosystem, incorporating the role of vegetation. Thus, the inventory and NUE estimates can be assumed *a priori* to differ due to those conceptual differences.

Statistics on countries

The regional NUE estimate for USA was made excluding Alaska and Hawaii (hence USA_{48}), since eddy-covariance flux sites do not characterize these areas climatologically. The population in 2010 was 306 675 006 [*U.S. Census Bureau,* 2012]. The area with an urban fraction of one in the aggregated 4 km scale data covers about 26 000 km^2 (Auxiliary Figure 2). Two NUE values were calculated for the European Union: one for the 25 member states prior to 2007 (EU_{25}) and one for the 27 member states at present (EU_{27}, Auxiliary Figure 1). The population of the EU in 2011 was 502 477 005 [*Eurostat,* 2012], and the area covered by complete urbanization is about 12 600 and 13 000 km^2 for EU_{25} and EU_{27}, respectively (Auxiliary Figure 2). Overall, USA has a higher occurrence of very densely built-up city centers whereas greener cities are more common in the EU. Furthermore, China has wide areas of low urban fraction which are shown as carbon sinks in Figure 3 of the main text. The area covered by complete urbanization is about the same in eastern China and Japan, about 5600 and 5700 km^2, respectively.

2. Auxiliary discussion

Relationship between population density and NUE

The annual NUE estimates from eddy-covariance flux measurements (Auxiliary Table 1) grow linearly with population density, though the correspondence is not as high as with natural fraction (Auxiliary Figure 5, $r^2 = 0.60$, rms = 1.13 kg C m^{-2} yr^{-1}). The dependency does not saturate with high population density, although fuel consumption is known to be inversely proportional to population density [*Kennedy et al.,* 2009; *Karathodorou et al.,* 2010]. This might be due to a lack of eddy-covariance measurements in areas with very high population density.

Regional estimates for NUE for North America and eastern Asia

The urban fraction ($f_u = 1 - f_n$) in North America and eastern Asia are depicted in Auxiliary Figures 4a and 5a. The annual NUE estimates, based on the relationship in Figure 1 in main text, for these regions are displayed in Auxiliary Figures 4b and 5b. For further discussion, see section 3.2 in the main text.

Auxiliary Table 1. Sites with annual CO_2 budgets measured with the eddy-covariance method, in chronological order. NUE is the urban ecosystem exchange (kg C m^{-2} yr^{-1}), f_n is the fraction of natural area around the measurement tower, R (m) is the radius of the circle for which f_n was determined, N is the amount of full days of data that the study has provided (taking into account the rejection of some data due to quality assurance), and gap-fill method gives the means of filling in of gaps in the CO_2 flux time series (GRNN—generalized regression neural networks, ANN—artificial neural networks). See references for further details on gap-filling methods. Only measurements lasting over a full year are included.

City	**Country**	**Source**	**NUE**	f_n	R	N	**Gap-fill method**
Tokyo	Japan	[*Moriwaki and Kanda,* 2004]	3.352	0.206	500	259	Look-up tables
Melbourne	Australia	[*Coutts et al.,* 2007]	2.317	0.380	500	256	GRNN
Essen, urban sector	Germany	[*Kordowski and Kuttler,* 2010]	4.284	0.220	1000	87[a]	ANN
Essen, park sector	Germany	[*Kordowski and Kuttler,* 2010]	2.138	0.520	1000	85[a]	ANN
Łódź	Poland	[*Pawlak et al.,* 2011]	2.947	0.400	500	414	Mean monthly fluxes
Minnesota	USA	[*Hiller et al.,* 2011]	0.136	0.938	70[b]	490	Light response during daytime, temperature during night-time
Baltimore	USA	[*Crawford et al.,* 2011]	0.361	0.674	1000	968	Light response during daytime, temperature during night-time
Montreal, urban	Canada	[*Bergeron and Strachan,* 2011]	5.567	0.290	1000	294	Average daily fluxes; interpolation
Montreal, suburban	Canada	[*Bergeron and Strachan,* 2011]	1.419	0.500	1000	372	Average daily fluxes; interpolation
London	UK	[*Helfter et al.,* 2011]	9.688	0.080	10000	329	Daily averages
Vancouver	Canada	[*Christen et al.,* 2011]	6.710	0.350	850[c]	511	Median diurnal cycles
Beijing	China	[*Song and Wang,* 2012]	5.622	0.120	2000	249	ANN

Florence	Italy	[*Gioli et al.,* 2012]	8.268	0.080	900[d]	1370	Mean diurnal cycles
Helsinki, semiurban	Finland	[*Järvi et al.,* 2012]	1.760	0.440	800	1060	ANN
Helsinki, semiurban road sector	Finland	[*Järvi et al.,* 2012]	3.500	0.410	800	97	ANN
Helsinki, semiurban vegetation sector	Finland	[*Järvi et al.,* 2012]	0.870	0.500	800	216	ANN
Helsinki, urban	Finland	[e]	4.740	0.113	1000	185	Median diurnal cycles

[a] data coverage is evaluated based on other information in the paper

[b] evaluated from Figure 1 in the paper for a 70-meter-radius circle around the tower

[c] for a rectangular area

[d] evaluated from Figure 1 in the paper for an area indicated in the figure with a mean radius of 900 m

[e] the NUE value calculated for a site described in [*Nordbo et al.,* Submitted to Boundary-Layer Meteorology, 2012] and using methods described in [*Järvi et al.,* 2012]

Auxiliary Table 2. Cities with annual GHG budgets, based on inventories. *P* is the population, *A* is the surface area (km^2), and the annual emissions are given as kg of carbon per person. The emission value corresponds to equivalents of CO_2 if other GHGs in addition to CO_2 are included in the inventory. The surface area is calculated from city border polygons [*GADM,* 2012]. Numbers after city names indicate multiple studies from the same urban area. Note that studies with same urban-area name may be for different areas (e.g. core city versus metropolitan area).

City	Country	Source	Study year	*P*	*A* (km^2)	Emissions (kg C yr^{-1} P^{-1})
Athens	Greece	[*Carney et al.,* 2009]	2005	3997006	3863	9.50
Bangkok 1	Thailand	[*Kennedy et al.,* 2009]	2005	5658953	1570	4.80
Bangkok 2	Thailand	[*Croci et al.,* 2011][a]	2007	5658953	1570	7.55
Barcelona	Spain	[*Kennedy et al.,* 2009]	2006	1605602	100	2.40
Beijing 1	China	[*Dhakal,* 2009]	2006	5810000	16388	9.00
Beijing 2	China	[*Sovacool and Brown,* 2010]	N/A	2000000	1360	4.33
Beijing 3	China	[*Wang et al.,* 2012]	2005	5380000	16388	8.62
Bologna	Italy	[*Carney et al.,* 2009]	2005	900000	3696	9.10
Brussels	Belgium	[*Carney et al.,* 2009]	2005	1006749	156	7.20
Chongqing 1	China	[*Dhakal,* 2009]	2006	8080000	82532	3.70
Chongqing 2	China	[*Wang et al.,* 2012]	2005	7980000	82532	2.88
Denver 1	USA	[*Ramaswami et al.,* 2008]	2005	579744	403	18.90
Denver 2	USA	[*Kennedy et al.,* 2009]	2005	579744	403	21.50
Denver 3	USA	[*Hillman and Ramaswami,* 2010]	2005	579744	403	17.88
District of Columbia	USA	[*Dodman,* 2009]	2005	573604	166	19.70

Frankfurt Rhein-Main	Germany	[*Carney et al.,* 2009]	2005	3761700	7371	12.65
Glasgow and Clyde Valley 1	UK	[*Dodman,* 2009]	2004	1747000	3365	8.40
Glasgow and Clyde Valley 2	UK	[*Carney et al.,* 2009]	2004	1750000	3365	7.34
Guangzhou	China	[*Wang et al.,* 2012]	2005	9580000	7153	7.86
Hamburg	Germany	[*Carney et al.,* 2009]	2005	4300000	19076	8.17
Hangzhou	China	[*Wang et al.,* 2012]	2005	7500000	17089	9.87
Helsinki 1	Finland	[*Carney et al.,* 2009]	2005	988500	762	6.70
Helsinki 2	Finland	[*Heinonen and Junnila,* 2011]	2006	550000	173	13.20
Lanzhou	China	[*Wang et al.,* 2012]	2005	3140000	13267	21.04
London 1	UK	[*Kennedy et al.,* 2009]	2003	7364100	1601	9.60
London 2	UK	[*Dodman,* 2009]	2006	7145161	1601	6.20
London 3	UK	[*Sovacool and Brown,* 2010]	N/A	8000000	1601	4.37
London 4	UK	[*Croci et al.,* 2011]	2003	7379700	1601	5.76
Los Angeles	USA	[*Kennedy et al.,* 2009]	2000	9519338	10590	13.00
Madrid 1	Spain	[*Carney et al.,* 2009]	2005	5938902	8022	6.28
Madrid 2	Spain	[*Croci et al.,* 2011]	2004	2938723	605	4.98
Milan	Italy	[*Croci et al.,* 2011]	2005	1298196	181	5.43
Nanjing 1	China	[*Bi et al.,* 2011]	2009	7713100	6592	9.78
Nanjing 2	China	[*Wang et al.,* 2012]	2005	6680000	6592	7.71
Oslo	Norway	[*Carney et al.,* 2009]	2005	1100000	5367	3.00
Osrednjeslovenska	Slovenia	[*Carney et al.,* 2009]	2005	492100	2540	8.77

Paris	France	[*Carney et al.,* 2009]	2005	1694000	12031	4.15
Porto	Portugal	[*Carney et al.,* 2009]	2005	1647000	1798	6.70
Porvoo	Finland	[*Heinonen and Junnila,* 2011]	2006	48000	656	10.30
Prague	Czech Republic	[*Kennedy et al.,* 2009]	2005	1181610	488	4.30
Rotterdam	The Netherlands	[*Carney et al.,* 2009]	2005	583000	264	29.20
Shanghai 1	China	[*Dhakal,* 2009]	2006	8150000	6890	12.60
Shanghai 2	China	[*Wang et al.,* 2012]	2005	7780000	6890	10.57
Shenyang	China	[*Wang et al.,* 2012]	2005	7400000	12872	6.68
Stockholm	Sweden	[*Carney et al.,* 2009]	2005	1950000	7145	3.20
Stuttgart	Germany	[*Carney et al.,* 2009]	2005	2700000	3650	15.00
Tianjin 1	China	[*Dhakal,* 2009]	2006	750000	11688	10.90
Tianjin 2	China	[*Wang et al.,* 2012]	2005	430000	11688	8.87
Tokyo 1	Japan	[*Sovacool and Brown,* 2010]	N/A	2800000	1801	5.98
Toronto 1	Canada	[*VandeWeghe and Kennedy,* 2007]	2001	600000	7619	8.15
Toronto 2	Canada	[*Kennedy et al.,* 2009]	2005	5555912	7619	8.20
Torino	Italy	[*Carney et al.,* 2009]	2005	2242775	6783	8.29
Veneto	Italy	[*Carney et al.,* 2009]	2005	4738313	17856	8.68
Wuhan	China	[*Wang et al.,* 2012]	2005	8580000	8386	13.84
Wuxi	China	[*Wang et al.,* 2012]	2005	5570000	4606	16.45
Zhengzhou	China	[*Wang et al.,* 2012]	2005	7160000	7521	9.24

[a] Population data were provided directly by the authors of this reference.

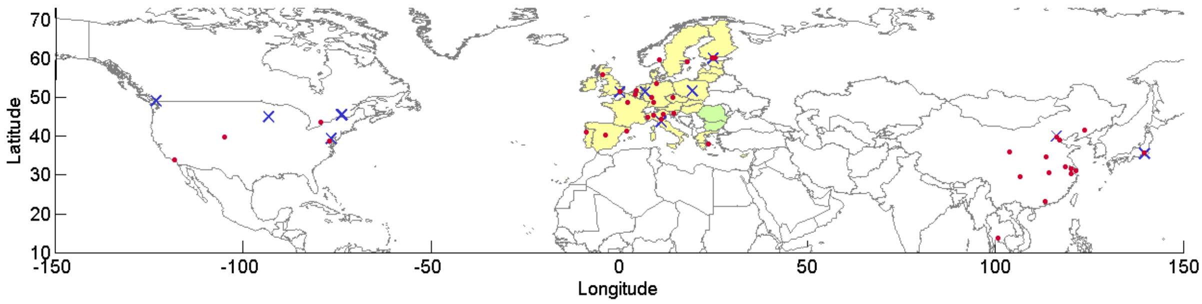

Auxiliary Figure 1. Locations of cities with eddy-covariance flux measurements in the northern hemisphere (blue crosses, Auxiliary Table 1) and of cities with GHG inventories (red dots, Auxiliary Table 2). Note that some sites overlap and thus the number of points on the map is not the same as the number of sites and cities in Auxiliary Table 1 and 2. The European Union with 25 member states (EU_{25}) is indicated with light yellow and the 2 states that joined 2007 (EU_{27}) are shown with light green.

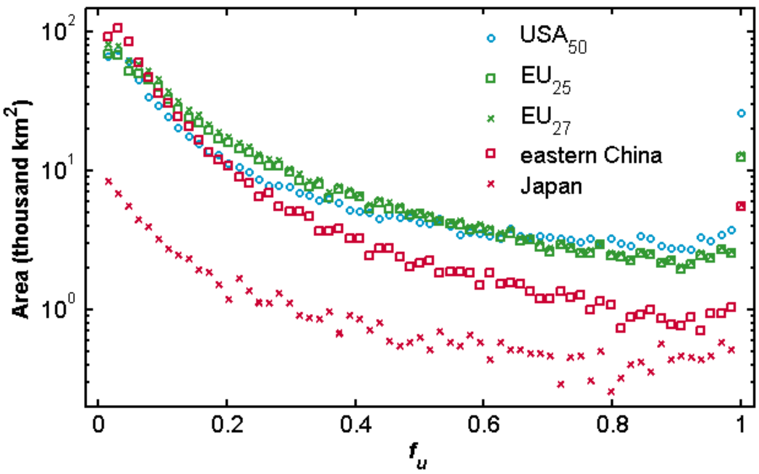

Auxiliary Figure 2. Area that is covered by a certain urban fraction (f_u) in USA_{48} (blue circle), EU_{25} (green square), EU_{27} (green cross), China (red squares, east of 105°E), and Japan (red crosses). One map pixel corresponds to an area of 16 km^2. There are 64 possible values of f_u.

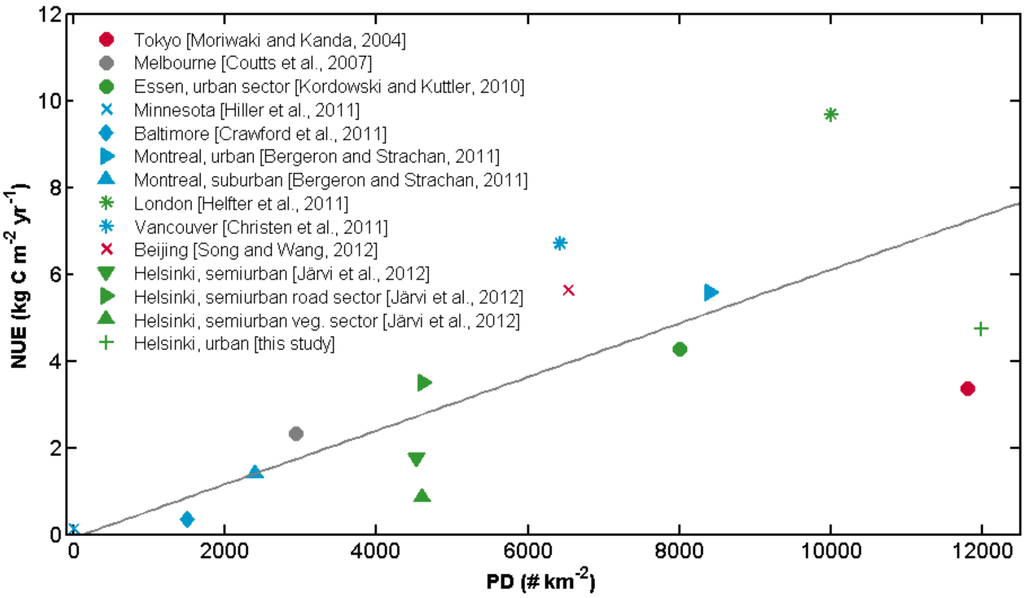

Auxiliary Figure 3. Net urban ecosystem exchange (NUE, kg C m^{-2} yr^{-1}) from direct flux measurements as a function of population density (PD, # km^{-2}). Continents are shown as colors: North America (blue), Europe (green), eastern Asia (red), Australia (gray). The weighted fit to all data is NUE = 6.18 10^{-4} kg C m^{-2} yr^{-1} km^2 PD –0.076 kg C m^{-2} yr^{-1}, N = 14, r^2 = 0.60, rms = 1.13 kg C m^{-2} yr^{-1}. Descriptions for data are given in Auxiliary Table 1. Note that all sites in Auxiliary Table 1 are not shown due to the lack of population-density data.

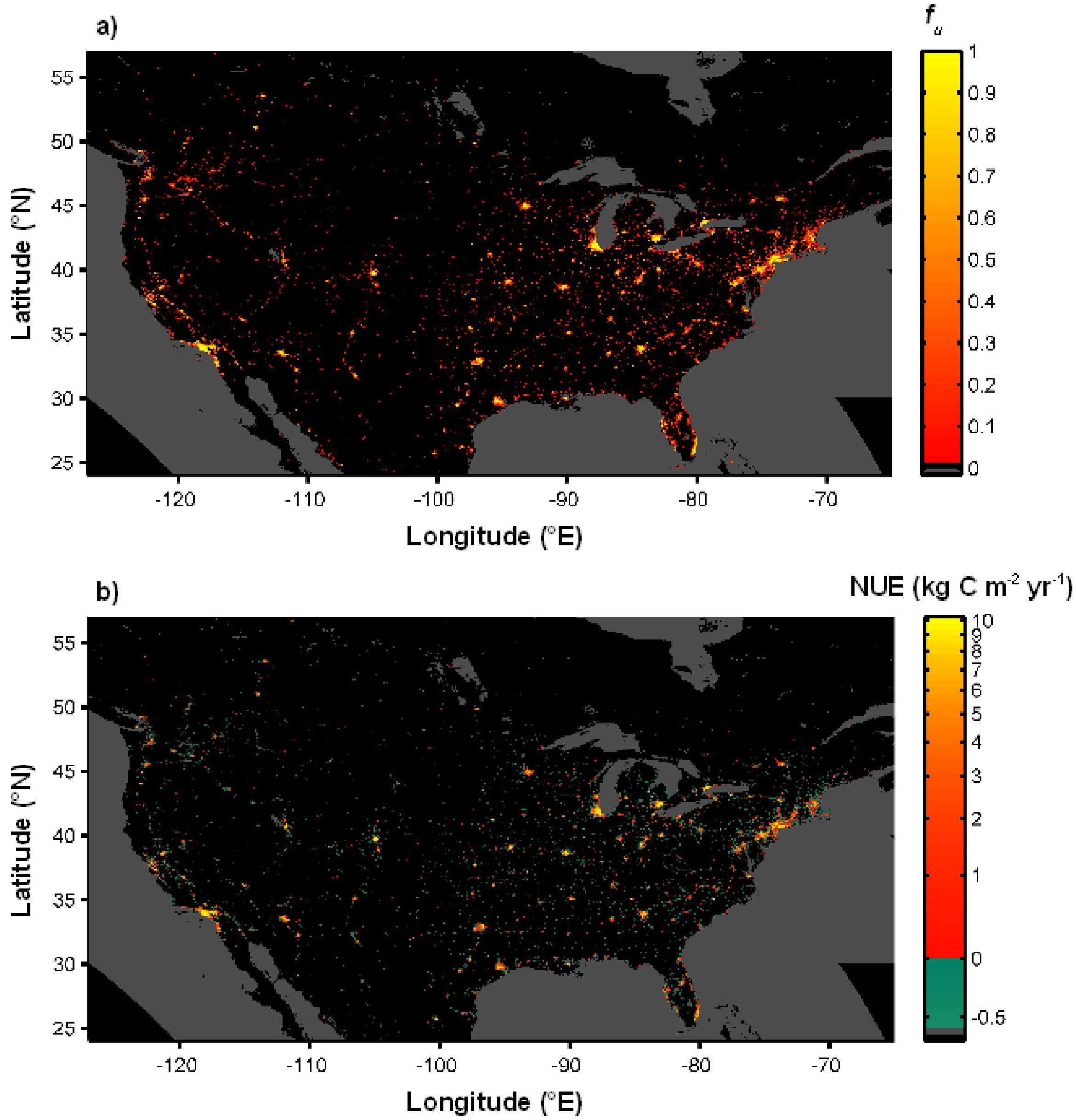

Auxiliary Figure 4. Urbanization and CO_2 budget in North America. a) Urban fraction (f_u) based on satellite observations, b) Net urban ecosystem exchange (NUE, kg C m^{-2} yr^{-1}) based on robust parameterization as a function of fraction of natural area (Figure 1 in main text). Black ocean shading shows missing data.

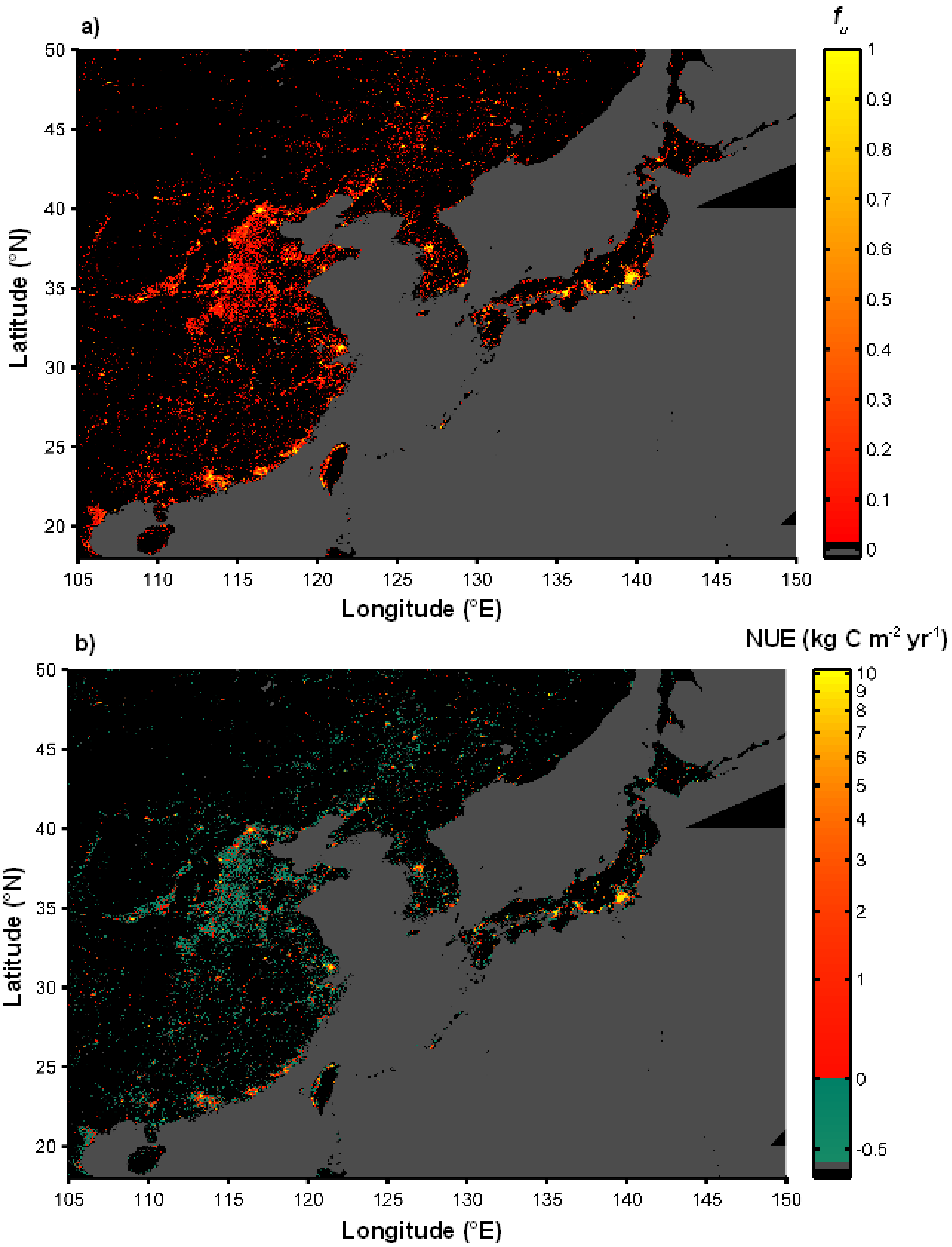

Auxiliary Figure 5. Urbanization and CO_2 budget in eastern Asia. a) Urban fraction (f_u) based on satellite observations, b) Net urban ecosystem exchange (NUE, kg C m^{-2} yr^{-1}) based on robust parameterization as a function of fraction of natural area (Figure 1 in main text). Black ocean shading shows missing data.

References

Bergeron, O. and I. B. Strachan (2011), CO2 sources and sinks in urban and suburban areas of a northern mid-latitude city*, Atmos. Environ., 45*, 1564-1573.

Bi, J., R. Zhang, H. Wang, M. Liu, and Y. Wu (2011), The benchmarks of carbon emissions and policy implications for China's cities: Case of Nanjing*, Energy Policy, 39*, 4785-4794.

Carney, S., N. W. Green R., and R. Read (2009), Greenhouse gas emissions inventories for 18 European regions, EU CO2 80/50 Project Stage 1: Inventory Formation.*, The Greenhouse Gas Regional Inventory Protocol (GRIP)*.

Christen, A., N. C. Coops, B. R. Crawford, R. Kellett, K. N. Liss, I. Olchovski, T. R. Tooke, M. van der Laan, and J. A. Voogt (2011), Validation of modeled carbon-dioxide emissions from an urban neighborhood with direct eddy-covariance measurements*, Atmos. Environ., 45*, 6057-6069.

Coutts, A. M., J. Beringer, and N. J. Tapper (2007), Characteristics influencing the variability of urban CO2 fluxes in Melbourne, Australia*, Atmos. Environ., 41*, 51-62.

Crawford, B., C. S. B. Grimmond, and A. Christen (2011), Five years of carbon dioxide fluxes measurements in a highly vegetated suburban area*, Atmos. Environ., 45*, 896-905.

Croci, E., S. Melandri, and T. Molteni (2011), Determinants of cities' GHG emissions: a comparison of seven global cities*, Int. J. Clim. Chang. Strateg. Manag., 3*, 275-301.

Dhakal, S. (2009), Urban energy use and carbon emissions from cities in China and policy implications*, Energy Policy, 37*, 4208-4219.

Dodman, D. (2009), Blaming cities for climate change? An analysis of urban greenhouse gas emissions inventories*, Environ. Urban., 21*, 185-201.

Eurostat (2012), Population at 1 January, http://epp.eurostat.ec.europa.eu/tgm/table.do?tab=table&language=en&pcode=tps00001&tableSelection=1&footnotes=yes&labeling=labels&plugin=1.

GADM (2012), Database of Global Administrative Areas, www.gadm.org.

Gioli, B., P. Toscano, E. Lugato, A. Matese, F. Miglietta, A. Zaldei, and F. P. Vaccari (2012), Methane and carbon dioxide fluxes and source partitioning in urban areas: The case study of Florence, Italy*, Environ. Pollut., 164*, 125-131.

Heinonen, J. and S. Junnila (2011), Case study on the carbon consumption of two metropolitan cities*, Int. J. Life Cycle Assess., 16*, 569-579.

Helfter, C., D. Famulari, G. J. Phillips, J. F. Barlow, C. R. Wood, C. S. B. Grimmond, and E. Nemitz (2011), Controls of carbon dioxide concentrations and fluxes above central London*, Atmos. Chem. Phys., 11*, 1913-1928.

Hiller, R. V., J. P. McFadden, and N. Kljun (2011), Interpreting CO2 Fluxes Over a Suburban Lawn: The Influence of Traffic Emissions*, Bound. -Layer Meteorol., 138*, 215-230.

Hillman, T. and A. Ramaswami (2010), Greenhouse Gas Emission Footprints and Energy Use Benchmarks for Eight US Cities*, Environ. Sci. Technol., 44*, 1902-1910.

Järvi, L., A. Nordbo, H. Junninen, A. Riikonen, J. Moilanen, E. Nikinmaa, and T. Vesala (2012), Seasonal and annual variation of carbon dioxide surface fluxes in Helsinki, Finland, in 2006-2010*, Atmos. Chem. Phys. Discuss., 12*, 8355-8396.

Karathodorou, N., D. J. Graham, and R. B. Noland (2010), Estimating the effect of urban density on fuel demand*, Energy Econ., 32*, 86-92.

Kennedy, C., J. Steinberger, B. Gasson, Y. Hansen, T. Hillman, M. Havranek, D. Pataki, A. Phdungsilp, A. Ramaswami, and G. Villalba Mendez (2009), Greenhouse Gas Emissions from Global Cities*, Environ. Sci. Technol., 43*, 7297-7302.

Kordowski, K. and W. Kuttler (2010), Carbon dioxide fluxes over an urban park area*, Atmos. Environ., 44*, 2722-2730.

MathWorks Inc , MATLAB*, 2012a*.

Moriwaki, R. and M. Kanda (2004), Seasonal and diurnal fluxes of radiation, heat, water vapor, and carbon dioxide over a suburban area*, J. Appl. Meteorol., 43*, 1700-1710.

Nordbo, A., L. Järvi, S. Haapanala, J. Moilanen, and T. Vesala (Submitted to Boundary-Layer Meteorology, 2012), Intra-city variation in urban morphology and turbulence structure in Helsinki, Finland.

Pawlak, W., K. Fortuniak, and M. Siedlecki (2011), Carbon dioxide flux in the centre of Łódź, Poland - analysis of a 2-year eddy covariance measurement data set, *Int. J. Climatol., 31*, 232-243.

Ramaswami, A., T. Hillman, B. Janson, M. Reiner, and G. Thomas (2008), A demand-centered, hybrid life-cycle methodology for city-scale greenhouse gas inventories, *Environ. Sci. Technol., 42*, 6455-6461.

Song, T. and Y. Wang (2012), Carbon dioxide fluxes from an urban area in Beijing, *Atmos. Res., 106*, 139-149.

Sovacool, B. K. and M. A. Brown (2010), Twelve metropolitan carbon footprints: A preliminary comparative global assessment, *Energy Policy, 38*, 4856-4869.

U.S. Census Bureau (2012), State & County QuickFacts, http://quickfacts.census.gov/qfd/states.

VandeWeghe, J. R. and C. Kennedy (2007), A spatial analysis of residential greenhouse gas emissions in the Toronto Census Metropolitan Area, *J. Ind. Ecol., 11*, 133-144.

Vesala, T., N. Kljun, Ü. Rannik, J. Rinne, A. Sogachev, T. Markkanen, K. Sabelfeld, T. Foken, and M. Y. Leclerc (2008), Flux and concentration footprint modelling: State of the art, *Environ. Pollut., 152*, 653-666.

Wang, H., J. Bi, R. Zhang, and M. Liu (2012), The carbon emissions of Chinese cities, *Atmos. Chem. Phys. Discuss., 12*, 7985-8007.